Real-Time Stochastic Optimization of Energy Storage Management Using Deep Learning-Based Forecasts for Residential PV Applications

Faeza Hafiz, *Member, IEEE*, M. A. Awal, *Student Member, IEEE*, Anderson Rodrigo de Queiroz, and Iqbal Husain, *Fellow, IEEE*

***Abstract*—A computationally proficient real-time energy management method with stochastic optimization is presented for a residential photovoltaic (PV)-storage hybrid system comprised of a solar PV generation and a battery energy storage (BES). Existing offline energy management approaches for day-ahead scheduling of BES suffer from energy loss in real time due to the stochastic nature of load and solar generation. On the other hand, typical online algorithms do not offer optimal solutions for minimizing electricity purchase costs to the owners. To overcome these limitations, we propose an integrated energy management framework consisting of an offline optimization model concurrent with a real-time rule-based controller. The optimization is performed in receding horizon with load and solar generation forecast profiles using deep learning-based long short term memory method in rolling horizon to reduce the daily electricity purchase costs. The optimization model is formulated as a multistage stochastic program where we use the stochastic dual dynamic programming algorithm in the receding horizon to update the optimal set point for BES dispatch at a fixed interval. To prevent loss of energy during optimal solution update intervals, we introduce a rule-based controller underneath the optimization layer in finer time resolution at the power electronics converter control level. The proposed framework is evaluated using a real-time controller-hardware-in-the-loop test platform in an OPAL-RT simulator. The proposed real-time method is effective in reducing the net electricity purchase cost compared to other existing energy management methods.**

***Index Terms*—Deep learning, energy management, energy storage, load forecast, real-time control, stochastic programming.**

Manuscript received July 14, 2019; revised November 8, 2019, December 7, 2019, and January 5, 2020; accepted January 14, 2020. Date of publication January 21, 2020; date of current version April 24, 2020. Paper 2019-ESC-0761.R3, presented at the 2019 IEEE Industry Applications Society Annual Meeting, Baltimore, MD USA, Sep. 29–Oct. 3, and approved for publication in the IEEE TRANSACTIONS ON INDUSTRY APPLICATIONS by the Energy Systems Committee of the IEEE Industry Applications Society. This work was supported by the National Science Foundation under Award EEC-0812121 for FREEDM Engineering Research Center and ABB Endowed Professorship in the Electrical and Computer Engineering Department, North Carolina State University. *(Corresponding author: Faeza Hafiz.)*

F. Hafiz is with the Department of Electrical and Computer Engineering, North Carolina State University, Raleigh, NC 27695 USA, and also with ABB Corporate Research Center, Raleigh, NC 27606 USA (e-mail: fhafiz@ncsu.edu).

M. A. Awal and I. Husain are with the Department of Electrical and Computer Engineering, North Carolina State University, Raleigh, NC 27695 USA (e-mail: mawal@ncsu.edu; ihusain2@ncsu.edu).

A. R. de Queiroz is with the Department of Decision Science, School of Business, North Carolina Central University, Durham, NC 27707 USA (e-mail: ardequei@ncsu.edu).

Color versions of one or more of the figures in this article are available online at https://ieeexplore.ieee.org.

Digital Object Identifier 10.1109/TIA.2020.2968534

NOMENCLATURE

Indices	
t	Index for time.
$\omega_{L,t}$	Generated scenario for load.
ω_t	Generated scenario for solar generation.
Sets	
$\Omega_{L,t}$	Set of generated scenario for load.
$\Omega_{\text{PV},t}$	Set of generated scenario for solar generation.
Parameters	
Δt	Time interval (min).
Q_b	Photovoltaic-based energy storage capacity (kWh).
η	Charger efficiency (%).
$P_{\text{PV},t}$	Solar generation at time period t (kW).
$P_{L,t}$	Load demand at time period t (kW).
$\underline{\text{SOC}_b}$	Minimum battery energy storage state of charge (%).
$\overline{\text{SOC}_b}$	Maximum battery energy storage state of charge (%).
$\overline{P_b^{ch}}$	Battery energy storage maximum charging power (kW).
$\underline{P_b^{\text{disch}}}$	Battery energy storage minimum discharging power (kW).
$\underline{P_b^{ch}}$	Battery energy storage minimum charging power (kW).
$\overline{P_b^{\text{disch}}}$	Battery energy storage maximum discharging power (kW).
T	Total time period (min).
Variables	
$\text{SOC}_{b,t}$	State of charge of energy storage at time period t.
$P_{b,t}^{ch}$	Battery energy storage charging power at time period t (kW).
$P_{b,t}^{\text{disch}}$	Battery energy storage discharging power at time period t (kW).
$P_{\text{def},t}$	Deferred solar energy at time period t (kW).
$P_{\text{grid},t}$	Load demand from grid at time period t (kW).
$P_{\text{com},t}$	Difference between stochastic dual dynamic programming-based charge and discharge command at time period t (kW).
$P_{rb,t}$	Rule-based controller command at time period t (kW).

I. INTRODUCTION

CLEAN energy footprint, decrease in production costs, and the availability of solar energy resources have ushered an

unprecedented tremendous growth of rooftop solar photo-voltaic (PV) installations over the last decade. However, the mismatch between the peak of solar PV generation and a typical household load obstructs the best utilization of solar resources. Moreover, the existing grid infrastructure poses a major challenge to accommodate large-scale back-feeding of power from distributed PV to the grid. A possible solution to maximize the utilization and efficiency of residential PV installations is to deploy battery energy storage (BES). A hybrid PV-storage installation at the residential level is further justified by the declining trend in energy storage price. In such hybrid systems, optimal energy management of the BES becomes imperative to maximize both the economic benefits for the residential customers and the utilization of available renewable generation.

Improved energy management of a BES depends on the accuracy of load and PV generation forecasts [1]. Overestimation or underestimation of forecasts of these profiles drives the optimization of energy management in the wrong directions [2]. For load and solar generation forecasting, different machine-learning algorithms have been employed utilizing historical data, such as support vector machine (SVM), decision trees, artificial neural network (ANN), recurrent neural network (RNN) [3]–[6], and others. These neural network-based tools suffer from slow learning rate, overfitting, and identification of optimal hyperparameter values. To overcome these challenges, deep learning-based forecasting models were proposed in [7] and [8] for forecasting the electricity demand. In [7], a deep learning algorithm was applied after clustering the load profiles based on seasons. However, the impact of holidays and weekdays was neglected in this research work. Long short term memory (LSTM)-based load prediction was proposed in [8] where different appliance patterns were considered as features. This method is computationally extensive, requiring huge data storage, which makes this approach infeasible for real-time applications. To leverage the available forecast electricity demand for optimization of energy management, a faster prediction is mandatory in rolling horizon.

Most offline energy management solutions for BES dispatch focus primarily on load balancing to account for the fluctuation of renewable generation and increase grid reliability [9]–[11], improve energy storage efficiency [12], and to minimize electricity bills [13]. These reported methods were validated considering load and PV profiles identical to forecasted day-ahead profiles. However, in reality, these profiles are stochastic in nature and depend on the variability of weather and user's preference [14]. Real-time BES energy management considering the uncertainty in solar generation was reported in [15]–[17]. In [15], the optimization of energy management was formulated as a Markov decision process (MDP) and solved through dynamic programming (DP). A chance-constrained stochastic optimization model was proposed to improve economic gain for a PV-based power plant in [16]. Stochastic dual DP (SDDP)-based optimization process was considered for residential users in [17]. Uncertainty in both load and solar generation were considered in [18]. However, the correlation between the uncertain load and generation profiles was ignored, but was leveraged to augment the offline forecast and optimization process in [19] and [20].

For real-time BES control, Lyapunov optimization approach was employed in [21]–[23]. In [24], a dynamic energy management system for smart grid was proposed using adaptive DP (ADP) and reinforcement learning to serve critical loads. These works were based on asymptotic analysis (i.e., infinite time horizon). In [25], an online algorithm was suggested considering finite horizon. However, expected future costs were not considered in this research. In [26], expected future cost was considered through receding horizon optimization to reduce power curtailment by minimizing forecast errors in renewable energy resources. Model predictive control (MPC) was developed to achieve the maximum net profit from the deregulated energy market in [27]. In [28], uncertainty was considered in forecasted profiles and a two-stage stochastic model was demonstrated. The stochastic model was solved through Benders' decomposition method. However, online optimization methods require update intervals of the order of tens of minutes which may lead to deferred solar energy or unnecessary discharge of storage in real systems.

The lack of energy management systems that can account for a realistic representation of uncertainties while simultaneously addressing forecast deviations in real time serves as the motivation to search for an integrated controller that optimizes energy and resource utilization. In this regard, we proposed and developed an integrated controller that employs an SDDP-based energy management strategy that updates the BES charge/discharge dispatch set point at a slower time scale utilizing the forecast profiles and a real-time rule-based controller operating at a much finer time resolution. The load and solar generation profiles are forecasted using an LSTM-based deep learning neural network algorithm. The integrated framework for real-time energy management considers the deviation from the forecast profiles in a real system due to uncertainties in load and solar generation, as well as the correlation among them, to calculate expected future costs in the receding horizon. The real-time feedback available from the power electronic converters used for interfacing the BES with household loads and the grid are utilized in the SDDP algorithm. Furthermore, the rule-based controller minimizes undesired energy loss due to variability in load or solar PV generation in between the update intervals from SDDP, which can range from minutes to tens of minutes in a system. The addition of the real-time control along with optimization improves utilization of both solar generation and energy storage. The method is validated in real time in a control hardware-in-the-loop (CHIL) platform. The developed prototype of real-time embedded system in OPAL-RT simulator ensures the effectiveness of the proposed method for real-system applications.

The reminder of this article is organized as follows. Section II demonstrates the proposed methodology for real-time energy management. Section III presents the simulation setup for the real-time environment. Section VI analyzes the performance of the algorithm. Section V concludes the article.

II. Integrated Energy Management

A residential solar PV-storage hybrid system managed by an energy management controller is shown in Fig. 1. Solar PV

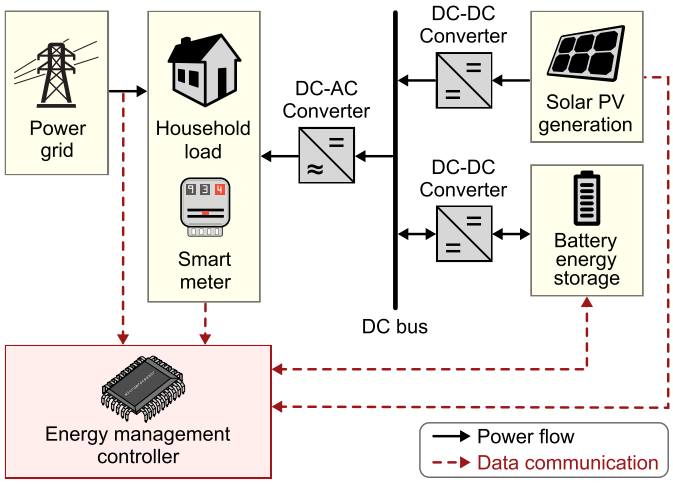

Fig. 1. Residential PV-storage hybrid system with power converters and energy management controller.

panels deliver energy to a BES unit and to satisfy the household electricity demand through a dc–dc converter and a dc bus. The BES is also connected to the dc bus through a dc–dc converter which can store energy only from the solar PV panels or discharge energy to meet the household demand. Therefore, household load is mitigated through the grid, solar panels, and/or BES unit. From dc bus, the household load is connected through a dc–ac converter.

In the proposed integrated energy management framework, three hierarchical steps are followed. In the first step, solar PV generation and load demand profiles for the next 24 h with 15-min resolution are forecasted. These updated forecasts are utilized to calculate the expected future costs in receding horizon in the second stage. Because of the stochastic nature of cloud patterns, weather, and user preference, solar generation and load demand do not maintain the forecast profiles. Optimization is performed considering these uncertainties of load and solar generation in the future. Utilizing the optimal set point to charge/discharge BES for next 15 min from the second stage, a rule-based control is performed in the third step. Since the proposed rule-based control takes less computation time, it can be implemented for real-time control purposes. The overview of the proposed three-step integrated energy management method is shown in Fig. 2. The description of each step is presented in the next subsections.

A. Step 1: Load and PV Generation Forecast

Incorporation of updated load and PV generation forecast profiles improves the optimal decision calculation of SDDP in receding horizon. In this integrated method, forecasts are performed at 15-min intervals considering previous stage historical data. To predict day-ahead profiles, the next 96 values for 24 h are forecasted. The considered features and forecasting algorithm are described as follows.

1) Feature Selection: Features are introduced in the algorithm to avoid overfitting/underfitting and increase the accuracy of the predicted values. For household electricity demand forecasts, the important features such as holiday or working day, month, day of the week, and previous 15 historical data are considered as features. These features help to predict the residents' electricity load patterns. Learning such patterns from the whole-house data with 1-min intervals introduces large prediction errors. Therefore, we consider forecasting load at a 15-min time interval [6].

2) Forecasting Algorithm: For forecasting, LSTM method is used, which is one of the RNN structures. In contrast to the standard, RNN is based on a series of repeating modules with relatively simple structure. Although a conventional feed-forward neural network can learn sequences, LSTM is more powerful because it constrains a memory cell in its structure to remember the important states in the past and has a forget gate to learn to reset the memory cell for the unimportant features during the learning process [29].

The simplest method to build up an LSTM model is to provide an input vector to the model for predicting the output. In this article, the LSTM network models are trained with an input vector of 17 features (weekday stamp, month stamp, and last 15 values of the time series) and the output window size is 96 which represents 24 h with 15-min interval. A way of training the LSTM models is to implement window-based learning. This method allows the LSTM model to directly deal with previous timestamp values (lagged values). After each prediction timestamp, LSTM window-based network model shifts both input and output windows by one step. In this way, the forecasted data provide support for dynamic learning.

B. Step 2: Optimization Problem Formulation

1) Scenario Generation: Since the forecast values cannot exactly predict the next day-ahead load and PV generation profiles due to the variability of the cloud and users' preference, uncertainties are required to be considered for enhancing the decision-making capabilities. In this work, the future uncertainties are modeled by developing a scenario tree to represent possible events for the random parameters. PV generation and household electricity demand are sampled from a probability distribution to construct this finite scenario tree independently.

We consider forecasts of PV generation and household electricity demand for the rolling horizon. For possible future scenarios, the correlation structure between solar generation and load profile is considered. After scenario generation for solar production and load demand independently from normal distributions $\mathcal{N}[\mu, \sigma^2]$, the correlation between them is incorporated through Cholesky decomposition. Following similar notation from [17] and [30], let K be the number of stages and n be the number of uncertain parameters. In this work, $n = 2$ since uncertainties in both solar PV generation and load demand are considered. Let X be a matrix $(K \times n)$ with independent distributed draws from a normal distribution $\mathcal{N}[0, 1]$ and R be the load and PV generation correlation matrix; the Cholesky decomposition of R will be a lower triangular matrix L as follows:

$$R = LL'. \tag{1}$$

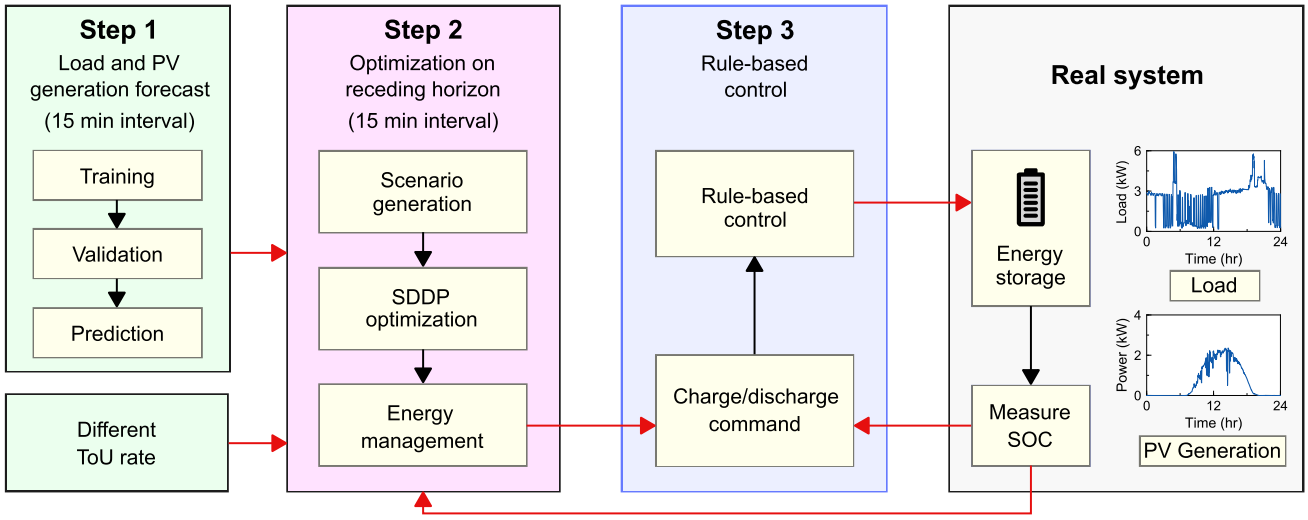

Fig. 2. Three-step protocol of the integrated energy management.

Correlated draws of Y matrix can be defined as

$$Y = LX \tag{2}$$

where Y corresponds to draws from $\mathcal{N}[0, \Sigma]$. The original draws are from $\mathcal{N}[0, 1]$, $\mu = 1$ and the covariance matrix is $\Sigma = R$. If correlated draws are used for solar PV generation and load demand scenario, given by $\mathcal{N}_{k,i}[\mu_i, \sigma_i^2]$ where $i = 1, 2$ at some stage t, draws from column i of Y can be multiplied by σ_i and mean μ_i is added. For instance, if $y_{k,i}$ is an element of the matrix Y corresponding to the ith draw, then scenario $(y_{k,i})$ will be generated as

$$\hat{y_{k,l}} = \mu_i + y_{k,i}\sigma_i. \tag{3}$$

In this method, it is possible to generate scenarios counting on the correlation effects among uncertain parameters. Since forecast PV generation will be zero during the night, generated PV scenarios will also be zero. Thus, load demand scenario will be generated directly from $\mathcal{N}[0, 1]]$ during the night.

Correlation consideration helps to avoid wrong scenario generation. For example, solar generation and atmospheric temperature become higher due to the intensity of the sun during summer days. Rising temperature increases the electricity load with the usage of air conditioners. If correlation is neglected, we might end up with a scenario such as higher solar generation and lower electricity demand for summer days.

2) Optimization Model Formulation: The overall objective is the household electricity purchase cost minimization with optimal operation of the energy storage integrated solar PV system. In this work, optimization cycle occurs from 0 to 24 h period of a day, with each 15-min interval in receding horizon. The total time left for a day after each cycle is divided into T time periods with resolution Δt, which is 15 min in this work. Let C_t be the ToU cost of electricity, $P_{L,t}^{\omega_{L,t}}$ and $P_{\text{PV},t}^{\omega_t}$ be the generated load and solar profiles from the sets of all generated load and solar profiles $\Omega_{L,t}$ and $\Omega_{\text{PV},t}$, respectively, and $P_{\text{grid},t}$ be the power demand from the grid at time t; the objective function and constraints can then be written as (4)–(12) in the following [31]:

$$J = \min\left(\sum_{t=1}^{T} C_t P_{\text{grid},t}\right) \tag{4}$$

subject to

power balance constraint

$$P_{\text{grid},t} - P_{b,t}^{ch} + P_{b,t}^{\text{disch}} - P_{def,t} = P_{L,t}^{\omega_{L,t}} - P_{\text{PV},t}^{\omega_t} \tag{5}$$

charge balance constraint

$$\text{SOC}_{b,t} = \text{SOC}_{b,t-1} + \frac{P_{b,t}^{ch}\Delta t\eta}{Q_b} - \frac{P_{b,t}^{\text{disch}}\Delta t}{Q_b\eta} \tag{6}$$

inequality constraints

$$P_{b,t}^{ch} \le P_{\text{PV},t}^{\omega_t}; t \in T \tag{7}$$

$$P_{b,t}^{\text{disch}} \le P_{L,t}^{\omega_{L,t}}; t \in T \tag{8}$$

$$P_{\text{grid},t} \ge 0; t \in T \tag{9}$$

upper and lower bounds of the decision variables

$$\underline{\text{SOC}_b} \le \text{SOC}_{b,t} \le \overline{\text{SOC}_b}; t \in T \tag{10}$$

$$\underline{P_b^{ch}} \le P_{b,t}^{ch} \le \overline{P_b^{ch}}; t \in T \tag{11}$$

$$\underline{P_b^{\text{disch}}} \le P_{b,t}^{\text{disch}} \le \overline{P_b^{\text{disch}}}; t \in T. \tag{12}$$

The PV-storage hybrid system considered in this research does not allow PV to backfeed into the grid. $P_{\text{def},t}$ will take care of the excess generation as deferred energy during periods of higher PV generation compared to the load demand with the storage fully charged. Equation (5) ensures the power balance of the whole system. Equation (6) calculates the state of charge (SOC) of storage $\text{SOC}_{b,t}$ based on the instantaneous charging $P_{b,t}^{ch}$ and the discharging power $P_{b,t}^{\text{disch}}$ of the storage device. Inequality constraints (7) maintain the condition that the storage will be charged only from the available PV generation, (8) ensures that storage discharging will occur only to mitigate the load

demand. Electricity purchases from grid will not be negative in (9) since backfeeding power to the grid is discouraged. The lower and upper bounds of the BES decision variables are defined in (10)–(12).

3) Multistage Stochastic Optimization: Model (4)–(12) described above considering uncertainty in solar PV generation and electricity demand can be represented as a T-stage stochastic linear program as follows:

$$h_t(x_{t-1}, b_t) = \min_{x_t} \left[c_t x_t + \mathbb{E}_{b_{t+1}|b_t} h_{t+1}(x_t, b_{t+1}) \right] \quad (13)$$

subject to

$$A_t x_t = B_t x_{t-1} + b_t : \pi_t \quad (14)$$

$$x_t \geq 0. \quad (15)$$

The decision variables of a particular stage t are considered in a vector x_t, which includes electricity purchases from the grid, power charge and discharge, and SOC levels for the storage devices. Parameter b_t represents the stochastic solar PV generation and load at stage t. In (13), $h_{t+1}(x_t, b_{t+1})$ is a recursive function that depends on decisions x_t made at stage t, and random parameters (load and PV generation) b_{t+1} are generated by the scenario tree at the beginning of stage $t+1$. Therefore, overall $\mathbb{E}_{b_{t+1}|b_t} h_{t+1}(x_t, b_{t+1})$ denotes the expected cost for the stage $t+1$, given that the stage t decisions and the random parameter realizations at that stage settled the initial conditions of the system at stage $t+1$. Equation (14) is the representation of power balance and charge balance constraints (5) and (6). Dual variables (denoted by π_t) derived from the transition constraints are used later to construct a piecewise linear approximation of the future cost function following Benders' decomposition scheme [32]. Equation (15) represents simple bounds on the decision variables such as (10)–(12). The realization of the random parameter b_{t+1} affects the condition of the system at stage t [33].

To solve the multistage stochastic program we employ the SDDP algorithm that constructs a piecewise linear approximation of the future costs function. A visualization of how the SDDP works to solve the multistage stochastic program is depicted in Fig. 3. It demonstrates the process for a simple three-stage problem. After obtaining the forecast profile as in Fig. 3(a), a scenario tree is generated similar to Fig. 3(b). The SDDP process is started by sampling forward paths (which are the highlighted paths) shown in Fig. 3(c) to proceed for the forward pass. During the forward pass, a sequence of models such as (13)–(15) [constructed considering (4)–(12)] is solved at each time stage using the simplex method. Benders' cuts are calculated during the backward pass and accumulated at each iteration for each stage. The set of updated cuts are later used as additional model constraints to better approximate the future costs and improve the decision-making process. To reach the desired convergence, the algorithm proceeds through a sequence of forward and backward passes, which is shown in Fig. 3(c) and (d), considering the updated representation of the Benders' cuts at each iteration [32], [33]. This algorithm does not discrete the state and decision spaces like DP, which results in less computation time and memory requirements. In the case of this work,

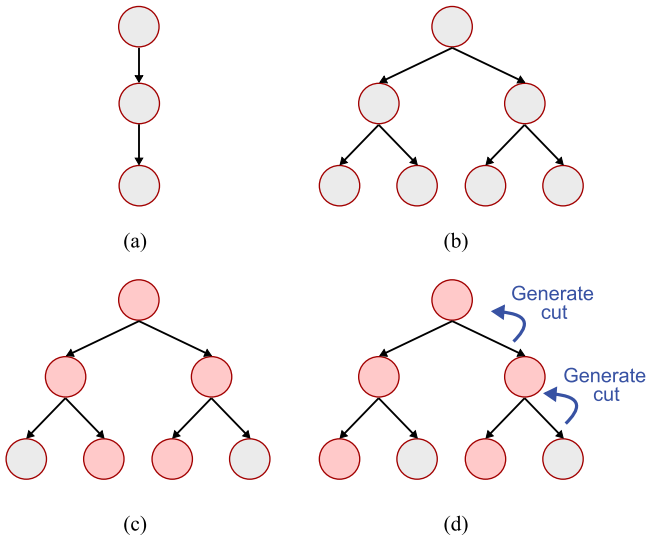

Fig. 3. SDDP solution process applied to a three-stage and two-scenarios-per-stage problem: (a) forecasted profile; (b) scenario tree generation; (c) forward pass through the highlighted paths; and (d) Benders' cut generation through backward pass.

the convergence of upper and lower bounds associated with the expected cost can be reached within a 15-min interval, given the complexity of the algorithm, which provides the lower bound for the update period. Additional discussions of the computation method and time requirement for SDDP can be found in [17] and [20], respectively.

C. Step 3: Rule-Based Control

The offline optimization strategy described in Section II-B alone for charging/discharging of the energy storage is not beneficial enough since there is the possibility of energy loss due to variability in load and/or solar PV generation in a real system with lower time resolution. A rule-based controller is integrated with the SDDP optimization method to further improve on the obtained optimal decisions from SDDP in real time. In the rule-based method, the optimization decisions $P_{\text{com},t}$ is calculated as (16) in the 15-min interval

$$P_{\text{com},t} = P_{b,t}^{ch} - P_{b,t}^{\text{disch}}. \quad (16)$$

If $P_{\text{com},t}$ is negative, then the BES should be discharged till the next update instant. If in real time, the load demand $P_{\text{load},t}$ is less than the discharge power $P_{b,t}^{\text{disch}}$, then the battery should discharge to mitigate the load. This rule is shown in Table I, steps 2–4. Here, P_{get} is the energy storage charge/discharge command for real time in significantly smaller intervals compatible with the power electronic converter sampling time (20 μs used in this work). On the other hand, if solar PV generation is higher than load in real time, then the optimization set point will be overruled to store excess PV generation in the BES based on its available capacity. This rule is illustrated in steps 5 and 6.

If $P_{\text{com},t}$ is positive, then the BES is supposed to be charged. If there is not enough solar PV generation $P_{\text{PV},t}$ to charge the BES in the real scenario, then $P_{b,t}^{ch}$ should be equal to the

TABLE I
RULE-BASED ALGORITHM

Inputs	$SOC_{real,t}$ at time, t
1	$P_{com,t} = P_{b,t}^{ch} - P_{b,t}^{disch}$
2	$if\ P_{com,t} \leq 0$ and $(P_{load,t} - P_{PV,t}) \geq 0$:
3	$if\ (P_{com,t} \geq P_{PV,t} - P_{load,t}) : P_{get} = P_{com,t}$
4	$else\ P_{get} = P_{PV,t} - P_{load,t}$
5	$elseif$: $P_{com,t} \leq 0$ and $(P_{load,t} - P_{PV,t}) \leq 0$:
6	$P_{get} = P_{PV,t} - P_{load,t}$
7	$elseif\ P_{com,t} \geq 0$ and $(P_{load,t} - P_{PV,t}) \geq 0$
8	$if\ P_{com,t} \leq P_{PV,t} : P_{get} = P_{com,t}$
9	$else\ P_{get} = P_{PV,t}$
10	$elseif\ P_{com,t} \geq 0$ and $(P_{load,t} - P_{PV,t}) \leq 0$
11	$P_{get} = P_{PV,t} - P_{load,t}$
12	$elseif\ P_{com,t} == 0$ and $(P_{load,t} - P_{PV,t}) \leq 0$
13	$P_{get} = P_{PV,t} - P_{load,t}$
14	$if\ P_{com,t} \leq \overline{P_{b,t}^{ch}}$: $P_{get} = \overline{P_{b,t}^{ch}}$
15	$else\ P_{get} = P_{com,t}$
16	$if\ SOC_{real,t} \leq \underline{SOC_b}$
17	$if\ P_{get} \geq 0 : P_{rb,t} = P_{get}$
18	$else : P_{rb,t} = 0$
19	$elseif : SOC_{real,t} \geq \overline{SOC_b}$:
20	$if\ P_{get} \leq 0 : P_{rb,t} = P_{get}$
21	$else : P_{rb,t} = 0$
22	$else$: $P_{rb,t} = P_{get}$

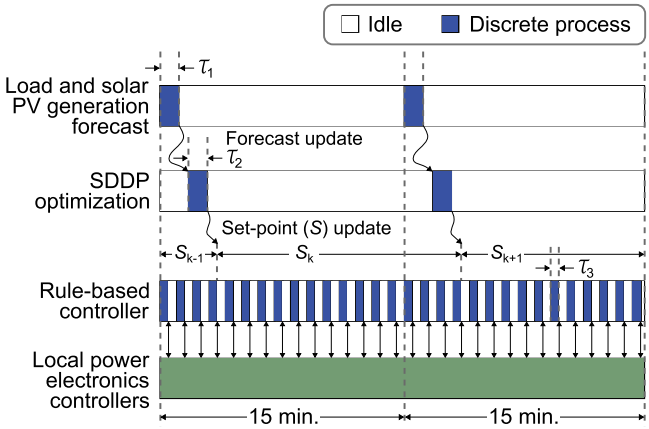

Fig. 4. Three-step protocol of the integrated energy management.

available $P_{\mathrm{PV},t}$. If there is higher $P_{\mathrm{PV},t}$ than $P_{\mathrm{load},t}$ and $P_{b,t}^{ch}$, then the excess generation is used to charge the BES considering available capacity. These rules are shown in Table I, steps 7–11.

If $P_{\mathrm{com},t}$ becomes zero, but still there is solar PV generation exceeding the load, then the BES should store the excess energy as long as it is within the charger capacity and the BES capacity bounds (steps 12–14). The rules and thresholds in steps 16–22 in Table I are set such that charge/discharge commands are disabled in real time if the upper/lower threshold limits of BES SOC are reached. $P_{rb,t}$ will be sent to the dc–dc converters of the BES from the controller.

The timing sequence of the proposed integrated energy management method is illustrated in Fig. 4. At each 15- min interval, the solar PV generation and load demand are forecasted for the next 24 h that takes τ_1 time to calculate. The forecasts are then used in the SDDP optimization process in the receding horizon requiring τ_2 time to update the optimal set points $P_{b,t}^{ch}$ and $P_{b,t}^{\mathrm{disch}}$. They will vary in each interval since the strategy

TABLE II
SYSTEM PARAMETERS

Parameters	Values
Q_b	4 kWh
$\underline{P_b^{ch}}$,$\overline{P_b^{ch}}$	0 kW, 3 kW
$\underline{P_b^{disch}}$,$\overline{P_b^{disch}}$	0 kW, 3 kW
Initial SOC_b	20%
$\underline{SOC_b}$,$\overline{SOC_b}$	20%, 80%
η	92%
Forecast and optimization time interval, t	15 min
Real-time simulation interval, τ	20μsec

TABLE III
TOU RATE

Season	Load Type	Period	ToU Rate ($/kWh)
Summer & Fall (June-September)	Off-peak	21:00-9:00	0.15
	Partial-Peak	10:00h-13:00h & 19:00h-21:00h	0.226
	Peak	13:00h-19:00h	0.342
Spring & Winter (October-May)	Off-peak	20:00-15:00	0.15
	Peak	17:00h-20:00h	0.17

defined by the SDDP algorithm will differ at each interval. These optimal set points are updated at every 15-min interval. For the BES real-time dynamic control, these updated optimal set points are provided to the rule-based controller considering (16). At each τ_3 time interval, the rule-based controller sends the charge/discharge command $P_{rb,t}$ to the BES considering real-time load demand and solar generation to avoid energy losses.

III. REAL-TIME SIMULATION SETUP

The proposed integrated energy management method is validated using a real-time simulation platform based on OPAL-RT. The solar PV, the BES, the household load, and the power converters are modeled in real time with a simulation time step of 20 μs. Household load and corresponding PV generation profiles are obtained from PECAN Street data [34]. In Table II, the test system parameters are given. The ToU rates have been collected from [35] and given in Table III. Forecasts and optimization are performed using MATLAB on a PC with an Intel Core i5-4600 U 1-GHz CPU, 4 GB of RAM, and 64-bit Windows 10 operating system. The OPAL-RT simulator is connected to the PC through a Modbus communication interface as shown in Fig. 5.

Using the SOC feedback from OPAL-RT, forecast and optimization are performed and new power set point for the BES is dispatched from PC to the OPAL-RT simulator at 15-min intervals. The rule-based controller is incorporated within the local power electronic converter controllers in the OPAL-RT simulator. The power converter models and controllers used for voltage and current tracking and the need of real-time CHIL simulation are described in the next subsections.

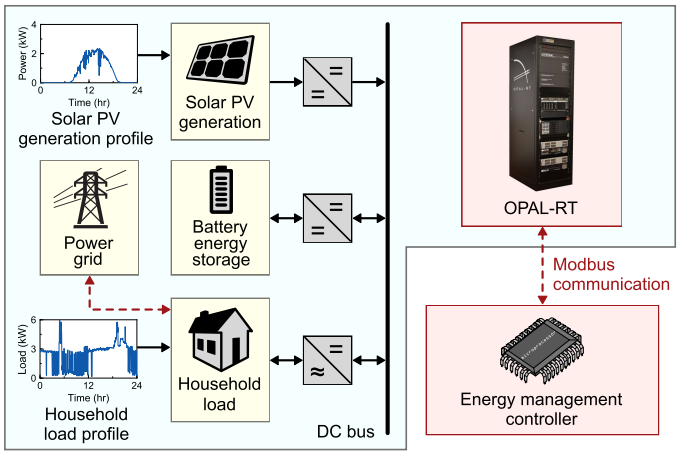

Fig. 5. Real-time simulation setup with Opal-RT.

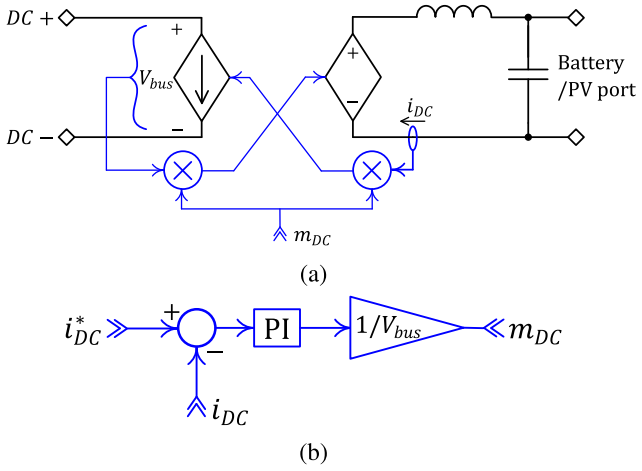

Fig. 6. (a) DC–DC converter model used for interfacing PV and battery. (b) Current controller for dc–dc converters.

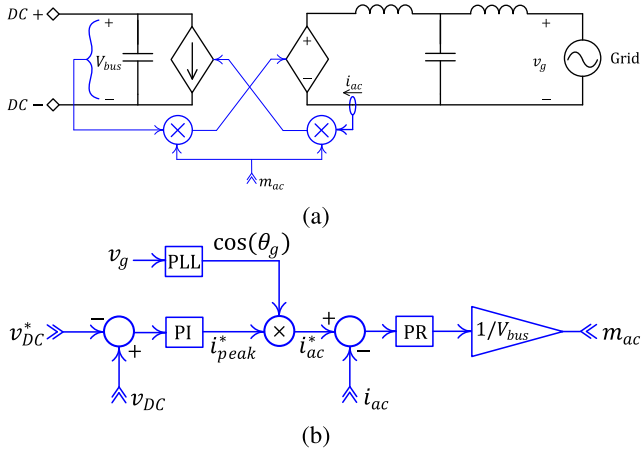

Fig. 7. (a) Grid interface rectifier model. (b) DC bus voltage and grid current controller used for the rectifier.

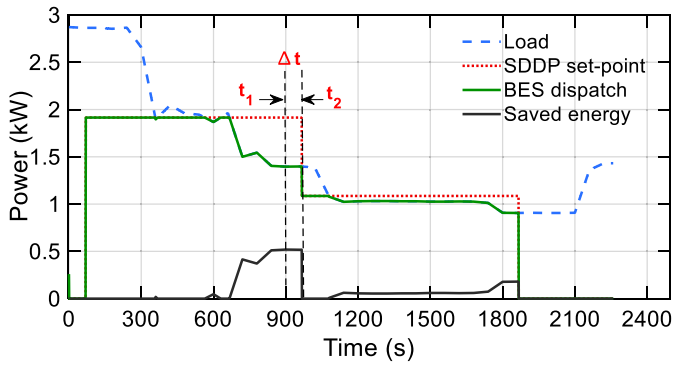

Fig. 8. Real-time CHIL simulation result showing the SDDP set point (updated at 15-min interval) and actual BES set point dispatched by rule-based controller. Simulation data were recorded at 1 s resolution.

A. Power Electronic Converter Model

To reduce the simulation overhead, average models of the power converters are used. Fig. 6(a) shows the average model used for the dc–dc converters. Identical models have been used for the converters that interface the solar PV and the BES. The converter current reference was tracked using a PI compensator as shown in Fig. 6(b). It is worth noting that the current reference $i^*_{\rm dc} = i^*_{\rm bat}$ for the dc–dc converter that interfaces the battery is updated by the rule-based controller. The current reference $i^*_{\rm dc} = i^*_{\rm PV}$ for the solar PV converter is also updated by the rule-based controller; however, the reference is tracked when allowable by the solar PV generation profile and the extracted current is clamped at the maximum power point when $i^*_{\rm PV} > i_{\rm MPP}$, where $i_{\rm MPP}$ refers to the current at maximum power point.

The average model of the power electronic rectifier that connects the household system with the grid is shown in Fig. 7(a). A cascaded control structure is used to maintain the desired voltage $v^*_{\rm dc}$ at the dc bus as shown in Fig. 7(b). An inner proportional-resonant (PR) compensator is used for current control and the peak current reference $i^*_{\rm peak}$ is dynamically generated by a PI compensator that tracks the dc bus voltage and a phase-locked-loop (PLL) is run on the grid voltage v_g to generate the reference phase θ_g.

B. Necessity of Real-Time CHIL Simulation

A real-time CHIL simulation facilitates a high-fidelity emulation of a real system. It provides an effective performance evaluation of any energy management algorithm compared to offline numerical simulations. This can be illustrated by a simple test case shown in Fig. 8, where a snapshot of the real-time CHIL experiment result is considered. The blue dashed curve represents the load. Stochastic nature of load demand is evident from the irregular variation of the curve. Battery power dispatch set point calculated from SDDP optimization is denoted by the red-dotted curve. This command is constant between two update instants, i.e., 15 min. It is worth noting that the load demand changes intermittently within the 15-min interval. The proposed rule-based controller limits the BES discharge when load demand falls below the set point. Thus, inclusion of rule-based controller on power electronics level with update interval of 20 μs ensures energy saving. This is evident in Fig. 8 where the energy saving over a 2400-s period is 307.5 kWh. In offline

numerical simulators, energy consumption and net energy output are typically computed considering the average power flow over one optimization-update period. As a result, the effect of intermittent mismatches between the commanded power reference and the varying load conditions leads to inaccuracies in the estimation of net cost.

Offline simulation executes forecasting and SDDP with rule-based controls in a synchronous way although the real-time process is asynchronous. Therefore, offline simulation leads to erroneous estimation of energy costs. A disadvantage of offline simulation is the inability to take into account the latency caused by computation and communication among controllers. The impact of such latency is evident in Fig. 8. The SOC feedback taken at t_1 is used to run the optimization algorithm and a new set point is available at t_2. The system keeps running using the previous set point till t_2. The delay time $\Delta t = t_2 - t_1$ accounts for the computation and the Modbus communication delays between the BES and the energy management controller. In an offline simulation using MATLAB, the entire system would be stopped at t_1 update instant while a new set point would be computed. The simulation would restart from t_1, completely ignoring the effect of the latency present in real systems.

IV. Simulation Results and Analysis

The simulation results for different steps and comparison analysis are presented next.

A. Load and Solar PV Generation Forecasts

For residential load and solar generation forecasts, we use load and PV generation data of the previous one-year period to train the model. The sampling rate of available Pecan Street data is 1 min. There are few missing values (approximately 1%) in electricity consumption data associated with the Pecan Street dataset used. The missing values are filled by inserting the mean values of the previous five time steps. The resolution of the datasets is reduced to 15 minute by aggregating values within each 15-min interval. Holiday's and weekday's information are extracted from [36]. For training the model, previous one-year data with 15-min resolution are considered. We used scikitlearn and Keras deep learning packages in Python to apply machine learning-based algorithms.

Lusisa *et al.* demonstrated that the smaller the interval, the larger is the forecast error [37]. Hence, a reasonable compromise is required in selecting the interval span to limit errors while meeting the algorithm computation time requirements. The time interval for forecast and optimization updates is chosen to be 15 min in our implementation based on the data availability in smart meters and allowing sufficient computation time for completing the SDDP process with the given resources. Accordingly, the prediction is updated at 15-min intervals in rolling horizon. Using the feedback of load and PV profiles in the current interval, prediction for the next 24 h, i.e., 96 sets of values, are updated. We evaluate different machine learning algorithms in terms of forecast accuracy. In Fig. 9, the forecast solar profiles with different algorithms along with the real profiles are shown. Load profile typically has higher variability compared to PV

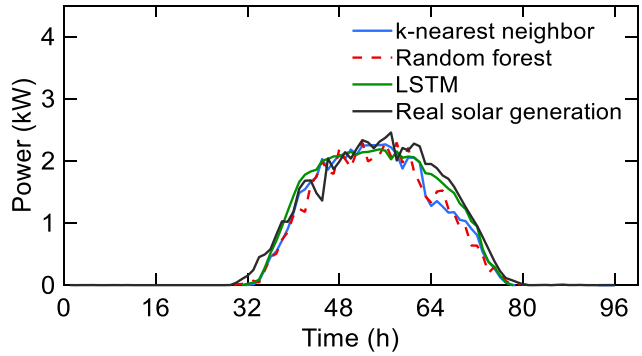

Fig. 9. Solar PV generation profile forecast.

TABLE IV
RMSE for Load and Solar Generation Forecasts

Forecasting methods	Solar forecast		Load forecast	
	Summer	Winter	Summer	Winter
k nearest neighbour	3%	5.8%	21%	14%
Random forrest algorithm	3.3%	6.4%	20%	13%
LSTM	2%	5.6%	17%	10%

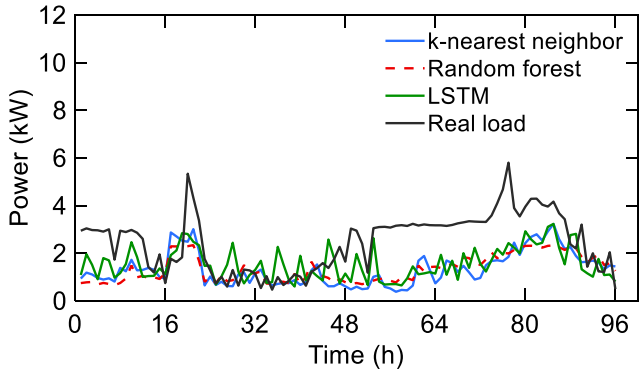

Fig. 10. Load demand profile forecast.

generation profile due to user preference which is reflected in the root-mean-square error (RMSE) shown in Table IV. A greater variability in household load demand is also evident in Fig. 10. Regardless, the RMSE is lower for LSTM compared to the other machine learning algorithms for both load demand and solar PV generation forecasts. A 15-min interval is chosen as a reasonable compromise for forecasts and optimization updates since RMSE increases as time resolution decreases.

B. Electricity Purchase Cost Reduction

The load and solar PV models in OPAL-RT real-time simulator are programmed to follow the profiles of a summer day (obtained from PECAN street data) as shown in Fig. 11. It is worth noting that the dataset used to train the forecast model does not include these profiles. The simulation results are recorded at 1-min interval for 24 h. The BES SOC for different control strategies are shown in Fig. 12 where it can be seen that the integrated energy management and the SDDP method prefer to charge during the off-peak and partial-peak hours and discharge

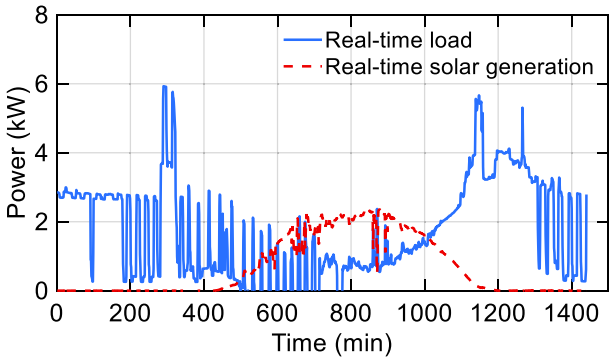

Fig. 11. Applied load and solar generation profiles in OPAL-RT simulator.

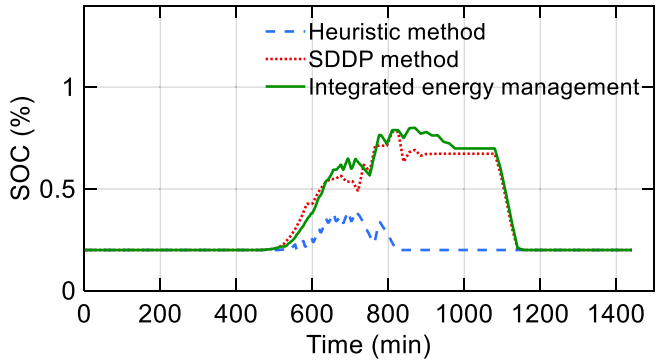

Fig. 12. SOC of the BES in real time for different control strategies on a summer day.

TABLE V
ELECTRICITY PURCHASE COST COMPARISON

Methods	Summer ($/day)	Winter ($/day)
Electricity purchase costs without storage	8.9	3.2
Heuristic method	8.4	3
SDDP method	8.5	3
Integrated energy management	7.9	2.9

mostly at peak hours to reduce the electricity purchase costs. As a result, SOC increases during off-peak and partial-peak hours and it goes down during peak hours. On the other hand, for heuristic method, the BES is always charged during periods of excess generation and discharged during periods of higher load than generation, which leads to under utilization of the BES. The proposed integrated algorithm is designed to manage the larger deviations between forecast and real data which happens in the 50th hour of the forecast data presented in Fig. 10. During periods of such large error in forecast, the SOC for the integrated energy management deviates from the SDDP-based optimization method as seen in Fig. 12.

Next, we evaluate the impact of the proposed integrated energy management with the SDDP method. The BES charging and discharging commands are updated at 15-min intervals from the SDDP method. Without the rule-based control, the mismatch of load and the SDDP optimization set point causes energy loss at finer time resolution based on Section IV.B. The results presented in Table V show that the integrated energy

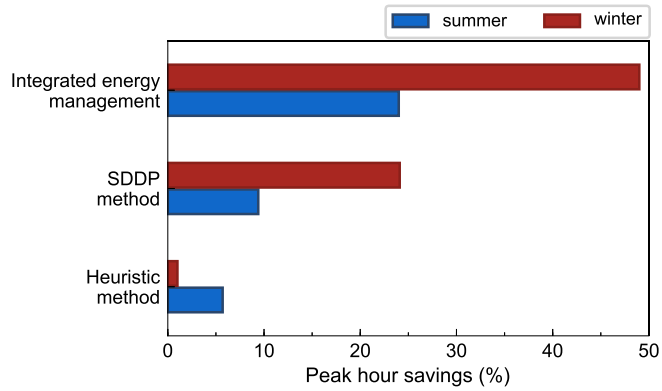

Fig. 13. Peak hour savings (in %) for different control strategies.

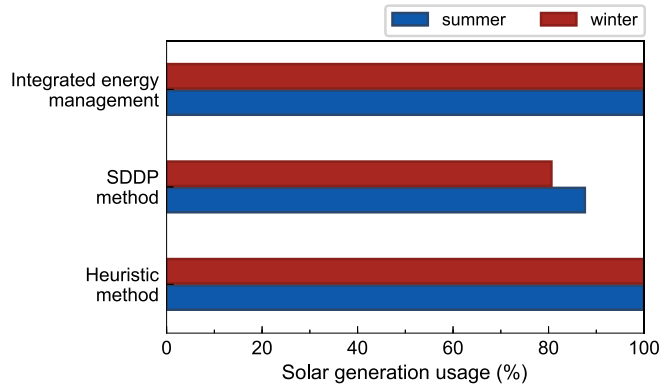

Fig. 14. Solar generation usage (in %) for different control strategies.

management controller ensures greater reduction in electricity purchase costs in both summer and winter days compared to the other methods. Electricity purchase cost savings are lower in winter days compared to summer days due to the lower solar PV generation and lower difference between the peak and off-peak hour ToU rates in winter. Considering these electricity purchase costs ($/day), it can be expected that the proposed integrated energy management can achieve 8.4% savings annually.

C. Peak Hour Savings and Solar Energy Usage

In our proposed method, peak hour savings is higher compared to the other methods for both summer and winter days which is shown in the bar chart in Fig. 13. Since the SDDP method has proper estimation of expected future cost, it ensures higher peak savings compared to the heuristic control method. But the SDDP-based control suffers from inefficient usage of solar PV energy due to the variability in real systems which is depicted in Fig. 14 for both summer and winter days. Peak hour savings not only help the homeowners but also the utility companies. The integrated energy management outperforms both the heuristic and the SDDP approaches in terms of peak hour savings and solar PV energy usage due to the integration of the SDDP for proper estimation of the expected future cost along with the rule-based control for efficient energy utilization.

V. Conclusion

In this article, a real-time residential BES energy management method is proposed for daily electricity purchase cost minimization of a homeowner with a PV-storage hybrid system. Updated load and solar generation profiles through forecasts in rolling horizon help to improve the optimal decision-making process in the energy management algorithm. Consideration of uncertain parameters and correlation between them increases the efficiency of the optimization. The integration of rule-based control reduces the solar energy loss and ensures proper utilization of the energy storage in a real system. Real-time CHIL experiments validate the superior performance of the integrated energy management in comparison with existing energy management algorithms in terms of electricity purchase cost, peak hour savings, and solar energy usage. The integrated energy management method developed in this work provides the baseline for extensions in community-based systems and gird-level analysis.

Acknowledgment

The authors would like to thank H. Yu from North Carolina State University for important discussions.

References

[1] W. He, "Load forecasting via deep neural networks," *Procedia Comput. Sci.*, vol. 122, pp. 308–314, 2017.

[2] W. C. Hong, Y. Dong, W. Y. Zhang, L. Y. Chen, and B. Panigrahi, "Cyclic electric load forecasting by seasonal SVR with chaotic genetic algorithm," *Int. J. Elect. Power Energy Syst.*, vol. 44, no. 1, pp. 604–614, 2013.

[3] Y. Chen, W. C. Hong, W. Shen, and N. Huang, "Electric load forecasting based on a least squares support vector machine with fuzzy time series and global harmony search algorithm," *Energies*, vol. 70, no. 9, pp. 1–13, 2016.

[4] G. Dudek, "Short-term load forecasting using random forests," in *Proc. Intell. Syst.*, 2015, pp. 821–828.

[5] A. Ahmad *et al.*, "A review on applications of ANN and SVM for building electrical energy consumption forecasting," *Renewable Sustain. Energy Rev.*, vol. 33, no. 1, pp. 102–109, 2014.

[6] J. Zheng, C. Xu, Z. Zhang, and X. Li, "Electric load forecasting in smart grids using long-short-term-memory based recurrent neural network," in *Proc. IEEE 51st Annu. Conf. Inf. Sci. Syst.*, 2017, pp. 1–6.

[7] J. Bedi and D. Toshniwal, "Empirical mode decomposition based deep learning for electricity demand forecasting," *IEEE Access*, vol. 6, pp. 49144–49156, 2018.

[8] W. Kong, Z. Y. Dong, D. J. Hill, F. Luo, and Y. Xu, "Short-term residential load forecasting based on resident behaviour learning," *IEEE Trans. Power Syst.*, vol. 33, no. 1, pp. 1087–1088, Jan. 2017.

[9] F. Hafiz, P. Fajri, and I. Husain, "Load regulation of a smart household with PV-storage and electric vehicle by dynamic programming successive algorithm technique," in *Proc. IEEE Power Energy Soc. General Meeting*, 2016, pp. 1–5.

[10] M. Zeraati, M. E. H. Golshan, and J. M. Guerrero, "A consensus-based cooperative control of PEV battery and PV active power curtailment for voltage regulation in distribution networks," *IEEE Trans. Smart Grid*, vol. 10, no. 1, pp. 670–680, Jan. 2017.

[11] S. Grillo, M. Marinelli, S. Massucco, and F. Silvestro, "Optimal management strategy of a battery-based storage system to improve renewable energy integration in distribution networks," *IEEE Trans. Smart Grid*, vol. 3, no. 2, pp. 950–958, Jun. 2012.

[12] J. Wu, X. Xing, X. Liu, J. M. Guerrero, and Z. Chen, "Energy management strategy for grid-tied microgrids considering the energy storage efficiency," *IEEE Trans. Ind. Electron.*, vol. 65, no. 12, pp. 9539–9549, Dec. 2018.

[13] X. Zhu, J. Yan, and N. Lu, "A graphical performance-based energy storage capacity sizing method for high solar penetration residential feeders," *IEEE Trans. Smart Grid*, vol. 8, no. 1, pp. 3–12, Jan. 2017.

[14] E. Ela, V. Diakov, E. Ibanez, and M. Heaney, "Impacts of variability and uncertainty in solar photovoltaic generation at multiple timescales," Nat. Renewable Energy Lab., Golden, CO, USA, Tech. Rep. NREL/TP-5500-58274, 2013.

[15] Y. Wang, X. Lin, and M. Pedram, "Adaptive control for energy storage systems in households with photovoltaic modules," *IEEE Trans. Smart Grid*, vol. 5, no. 2, pp. 992–1001, Mar. 2014.

[16] F. Conte, S. Massucco, M. Saviozzi, and F. Silvestro, "A stochastic optimization method for planning and real-time control of integrated PV-storage systems: Design and experimental validation," *IEEE Trans. Sustain. Energy*, vol. 9, no. 3, pp. 1188–1197, Jul. 2018.

[17] F. Hafiz, A. R. de Queiroz, and I. Husain, "Multi-stage stochastic optimization for a PV-storage hybrid unit in a household," in *Proc. IEEE Ind. Appl. Soc. Annu. Meeting*, 2017, pp. 1–7.

[18] A. Mohamed, V. Salehi, and O. Mohammed, "Real-time energy management algorithm for mitigation of pulse loads in hybrid microgrids," *IEEE Trans. Smart Grid*, vol. 3, no. 4, pp. 1911–1922, Dec. 2012.

[19] M. Nistor and C. H. Antunes, "Integrated management of energy resources in residential buildings—A Markovian approach," *IEEE Trans. Smart Grid*, vol. 9, no. 1, pp. 240–251, Jan. 2018.

[20] F. Hafiz, A. R. de Queiroz, and I. Husain, "Coordinated control of PEV and PV-based storage system under generation and load uncertainties," in *Proc. IEEE Ind. Appl. Soc. Annu. Meeting*, 2018, pp. 1–5.

[21] T. Li and M. Dong, "Real-time energy storage management with renewable integration: Finite-time horizon approach," *IEEE J. Sel. Areas Commun.*, vol. 33, no. 12, pp. 2524–2539, Dec. 2015.

[22] T. Li and M. Dong, "Real-time residential-side joint energy storage management and load scheduling with renewable integration," *IEEE Trans. Smart Grid*, vol. 9, no. 1, pp. 283–298, Jan. 2018.

[23] W. Shi, N. Li, C. C. Chu, and R. Gadh, "Real-time energy management in microgrids," *IEEE Trans. Smart Grid*, vol. 8, no. 1, pp. 228–238, Jan. 2017.

[24] G. K. Venayagamoorthy, R. K. Sharma, P. K. Gautam, and A. Ahmadi, "Dynamic energy management system for a smart microgrid," *IEEE Trans. Neural Netw. Learn. Syst.*, vol. 27, no. 8, pp. 1643–1656, Aug. 2016.

[25] C. Chau, G. Zheng, and M. Chen, "Cost minimizing online algorithms for energy storage management with worst-case guarantee," *IEEE Trans. Smart Grid*, vol. 7, no. 6, pp. 2961–2702, Nov. 2016.

[26] A. Damiano, G. Gatto, I. Marongiu, M. Porru, and A. Serpi, "Real-time control strategy of energy storage systems for renewable energy sources exploitation," *IEEE Trans. Sustain. Energy*, vol. 5, no. 2, pp. 567–576, Apr. 2014.

[27] H. H. Abdeltawab and Y. A. R. Mohamed, "Market-oriented energy management of a hybrid wind-battery energy storage system via model predictive control with constraint optimizer," *IEEE Trans. Ind. Electron.*, vol. 62, no. 11, pp. 6658–6670, Nov. 2015.

[28] J. Soares, B. Canizes, M. A. F. Ghazvini, Z. Vale, and G. K. Venayagamoorthy, "Two-stage stochastic model using benders' decomposition for large-scale energy resource management in smart grids," *IEEE Trans. Ind. Appl.*, vol. 53, no. 6, pp. 5905–5914, Nov./Dec. 2017.

[29] F. A. Gers, N. N. Schraudolph, and J. Schmidhuber, "Learning precise timing with LSTM recurrent networks," *J. Mach. Learn. Res.*, vol. 3, pp. 115–143, 2002.

[30] S. R. Silva, A. R. de Queiroz, L. M. Lima, and J. W. Lima, "Effects of wind penetration in the scheduling of a hydro-dominant power system," in *Proc. IEEE PES General Meeting Conf. Expo.*, 2014, pp. 1–5.

[31] F. Hafiz, M. Awal, A. R. de Queiroz, and I. Husain, "Real-time stochastic optimization of energy storage management using rolling horizon forecasts for residential PV applications," in *Proc. IEEE Ind. Appl. Soc. Annu. Meeting*, 2019, pp. 1–9.

[32] M. V. Pereira and L. M. Pinto, "Multi-stage stochastic optimization applied to energy planning," *Math. Program.*, vol. 52, no. 1/3, pp. 359–375, 1991.

[33] A. R. de Queiroz and D. P. Morton, "Sharing cuts under aggregated forecasts when decomposing multi-stage stochastic programs," *Oper. Res. Lett.*, vol. 41, no. 3, pp. 311–316, 2013.

[34] *Household Load and Solar Generation Data*. (2016). [Online]. Available: http://www.pecanstreet.org

[35] *Time of Use Rates*. (2018). [Online]. Available: http://www.pge.com

[36] *US Federal Government Holiday Calendar*. (2018). [Online]. Available: https://kite.com/python/docs/pandas.tseries.holiday.USFederalHolidayCalendar

[37] P. Lusisa, K. R. Khalilpoura, L. Andrewa, and A. Liebmana, "Short-term residential load forecasting: Impact of calendar effects and forecast granularity," *Appl. Energy*, vol. 205, pp. 654–669, 2017.

Faeza Hafiz (Member, IEEE) received the B.Sc. and M.Sc. degrees in electrical and electronic engineering from the Bangladesh University of Engineering and Technology, Dhaka, Bangladesh, and the Ph.D. degree from the Department of Electrical and Computer Engineering, North Carolina State University, Raleigh, NC, USA.

She is a Research Scientist with ABB Corporate Research Center, Raleigh, NC, USA. Her research interests include home energy management, intelligent energy management systems for plug-in electric vehicles, smart grid, and optimization in power system.

M. A. Awal (Student Member, IEEE) received the bachelor's degree in electrical and electronic engineering from the Bangladesh University of Engineering and Technology, Dhaka, Bangladesh. He is currently working toward the Ph.D. degree with the Future Renewable Electric Energy Delivery and Management (FREEDM) Systems Center, North Carolina State University, Raleigh, NC, USA.

His research interests include converter level and system level control strategies for microgrids and networked power electronics systems.

Anderson Rodrigo de Queiroz received the B.Sc. and M.Sc. degrees in electrical engineering from the Federal University of Itajubá, Itajubá, Brazil, in 2005 and 2007, respectively, and the Ph.D. degree in operations research (OR) from the University of Texas at Austin, Austin, TX, USA, in 2011.

He is an Assistant Professor with the Department of Decision Sciences, North Carolina Central University (NCCU), Durham, NC, USA, and an Adjunct Research Professor with CCEE Department, North Carolina State University, Raleigh, NC, USA. Prior to joining NCCU, he was a Professor, Consultant, and Researcher. His research interests include OR, with focus on large-scale stochastic optimization, analytics, and decision-making techniques, as well as planning, operations, economics, and design of electrical and energy systems.

Iqbal Husain (Fellow, IEEE) received the Ph.D. degree in electrical engineering from Texas A&M University, College Station, TX, USA, in 1993.

He is the Director of FREEDM NSF Engineering Center and ABB Distinguished Professor with the Department of Electrical and Computer Engineering, North Carolina State University, Raleigh, NC, USA. Prior to joining NC State, he was with the University of Akron, Akron, OH, USA, where he built a successful power electronics and motor drives program. In 2001, he was a Visiting Professor with Oregon State University, Corvallis, OR, USA. His expertise is in the areas of power electronics, electric machines, motor drives, and system controls. The primary applications of his work are in the transportation, automotive, aerospace, and power industries. He has also developed innovative graduate and undergraduate courses on electric and hybrid vehicles. He is the Author of the textbook *Electric and Hybrid Vehicles: Design Fundamentals* (CRC Press, 2003) on this topic. His research interests include power electronics integration into power and transportation systems.

Dr. Husain was the recipient of the 2006 SAE Vincent Bendix Automotive Electronics Engineering Award, the 2004 College of Engineering Outstanding Researcher Award, the 2000 IEEE Third Millennium Medal, and the 1998 IEEE-IAS Outstanding Young Member Award. He is the Editor-in-Chief for the IEEE ELECTRIFICATION MAGAZINE.